State of platinum in zirconia and sulfated zirconia catalysts

Ram Srinivasan, Dennis E. Sparks and Burtron H. Davis

Center for Applied Energy Research, University of Kentucky, 3572 Iron Works Pike, Lexington, KY 40511, USA

Received 31 January 1996; accepted 3 May 1996

Platinum is present in a metallic state following activation in air at 725°C of both 5 wt% Pt/ZrO_2 and 5 wt% $Pt/SO_4^{2-}/ZrO_2$. Reduction of either catalyst at 725°C produces a Pt–Zr alloy, and these reduced catalysts, upon recalcination in air at 725°C, form metallic Pt crystallites. Likewise, reduction of these uncalcined catalysts at 725°C in H_2 leads to a Pt–Zr alloy formation. However, treatment of these uncalcined catalysts in H_2 at 450°C does not produce Pt crystallites large enough to detect by XRD.

Keywords: sulfated zirconia; platinum; X-ray diffraction; Pt–Zr alloy; zirconia alloy

1. Introduction

Sulfated zirconia attracts much attention as it is widely used for various reactions at low temperatures (e.g., refs. [1–4]). One of the main advantages of using SO_4^{2-}/ZrO_2 catalysts is that they have high activity at relatively low temperatures. Also, these catalysts, being solids, exhibit environmental advantages over strong liquid acids such as HF and H_2SO_4.

The presence of a noble metal (usually platinum) in SO_4^{2-}/ZrO_2 greatly enhances catalytic performance during the skeletal isomerization of alkanes [5,6] and improves the life of the catalyst. Thus, the state of platinum in these sulfated ZrO_2 catalysts is of interest.

Various characterization techniques have been used to define the state of platinum in these catalysts. An IR study of CO adsorbed on $Pt/SO_4^{2-}/ZrO_2$ showed no bands corresponding to adsorbed CO molecules [4,6]. Results from XPS studies of these catalysts [7–11] indicated that both Pt metal and Pt cations were present in the hydrogen-treated $Pt/SO_4^{2-}/ZrO_2$, with the binding energy of the Pt 4f electrons of the sulfated ZrO_2 catalyst being lower than that of the Pt 4f electrons in Pt/ZrO_2 [11]. It has been suggested that the Pt was covered with sulfur in $Pt/SO_4^{2-}/ZrO_2$ catalysts [12,13]. Paál et al. [12] suggested that the larger Pt particles are predominantly in the metallic state. However, line broadening and BE shifts due to inhomogeneous charging may mislead one to conclude otherwise. Paál et al. [12] also concluded that the loss of metallic character by Pt can be due to the presence of large surface PtS islands. However, Ebitani et al. [14] reported data to show that most of the platinum was present in a cationic state after reduction in H_2 at temperatures below 673 K. Sayari et al. [15] reported that platinum was present in the metallic state after activation in air at about 725°C, and suggested that a sulfur species acted to reduce platinum. High temperature X-ray diffraction studies showed that metallic platinum was present following calcination in air at high temperatures (> 700°C) [16]. EXAFS data [17] were interpreted to show that a considerable amount of unreduced Pt remains after reduction, and it was suggested that this was due to strong metal support interaction (SMSI) between Pt and ZrO_2. In contrast, the results of another EXAFS study [18] revealed the presence of metallic platinum in the catalyst following activation at 725°C for 2 h in air as well as after use as a catalyst.

In spite of intensive research in this area, the definition of the state of platinum is still elusive, and is therefore of great scientific interest.

Platinum is typically present as low as 0.6 wt% in the SO_4^{2-}/ZrO_2 catalyst, and this may present difficulties in obtaining experimental data. Therefore, both 0.6 wt% Pt and 5 wt% platinum loadings were used in this investigation of sulfated and unsulfated zirconias and various treatments were carried out in order to define the state of platinum in the working catalysts. In this communication, we describe XRD data that support the formation of metallic platinum in Pt/ZrO_2 catalysts and show evidence for interaction between Pt and ZrO_2.

2. Experimental

Hydrous ZrO_2 was rapidly precipitated at a pH of 10.5 by admixing 0.3 M $ZrCl_4$ solution and excess of NH_4OH base. The mixture was vigorously stirred and washed thoroughly [19] until a negative test for Cl^- ions was obtained for the filtrate. The washed precipitate was dried at 110°C overnight and the dried flakes were crushed to fine powders, which were again dried at 110°C overnight. This was sulfated using 0.5 M H_2SO_4 (15 ml/g of ZrO_2). The required amount of the catalyst was immersed in an appropriate amount of H_2SO_4, stirred for 2 h, and the sulfated ZrO_2 powders were then dried at 110°C. The sulfur content of the dried sample was in the range of 3.0–3.5 wt%. Both the precipitated

ZrO_2 and sulfated zirconia were impregnated with 0.6 wt% Pt and 5 wt% Pt using a H_2PtCl_6 salt solution.

Portions of these catalysts, namely Pt/ZrO_2 and $Pt/SO_4^{2-}/ZrO_2$, were activated at 725°C for 2 h in air. Several other portions were reduced at either 450 or 725°C for 6 h. After reduction at these temperatures in H_2, the catalysts were cooled to room temperature in H_2 and passivated for 25 h in 1% O_2–He mixture. After passivation, these catalysts were exposed to atmosphere and XRD was carried out.

For XRD, a Rigaku X-ray diffractometer was used. Cu Kα radiation was used at 40 kV, 20 mA, with a pyrolytic graphite in the diffracted beam path. Data were collected using a step size of 0.02° (sometimes 0.01°) with a count time of 2 s per step.

Differential thermal analysis (DTA) and thermogravimetric analysis (TGA) were conducted simultaneously using a Seiko TG/DTA 320 instrument. This unit has an operating range of 25–1200°C. The runs were conducted in helium as well as in a mixture of He/H_2 or He/air. For the runs conducted in helium, a flow rate of 200 ml/min was used. For the runs conducted with a mixture of gases, the helium flow was 150 ml/min from one gas inlet port, and the flow of the other gas (air or H_2) was 100 ml/min through another gas inlet port. Platinum pans were used as sample holders and sintered Al_2O_3 was used as the reference material. The heating rate was 20°C/min. The TG/DTA unit was connected to a disk station that performed tasks, such as programmable heating and cooling cycles, continuous weight measurements, sweep gas valve switching and data storage and analysis.

3. Results and discussion

The precipitated zirconia catalysts are amorphous to X-rays indicating a lack of ordered atomic orientation. Commonly, these catalysts are activated prior to use as a catalyst for hydrocarbon isomerization or cracking reactions. While the exact temperature of activation varies among laboratories, we have found that the optimum temperature may vary with each catalyst batch even when the preparative procedures are apparently the same. The precipitated catalysts, after sulfation using sulfuric acid, contained about 3.2 wt% S, and after activation at 725°C in air this amount was reduced to about 1 wt%.

The DTA curves are given in fig. 1 for the two catalysts when heated in helium, air and in hydrogen. The temperatures for crystallization are different for these two catalysts in these environments. For the 5 wt% $Pt/SO_4^{2-}/ZrO_2$ catalyst, the exotherm temperatures are

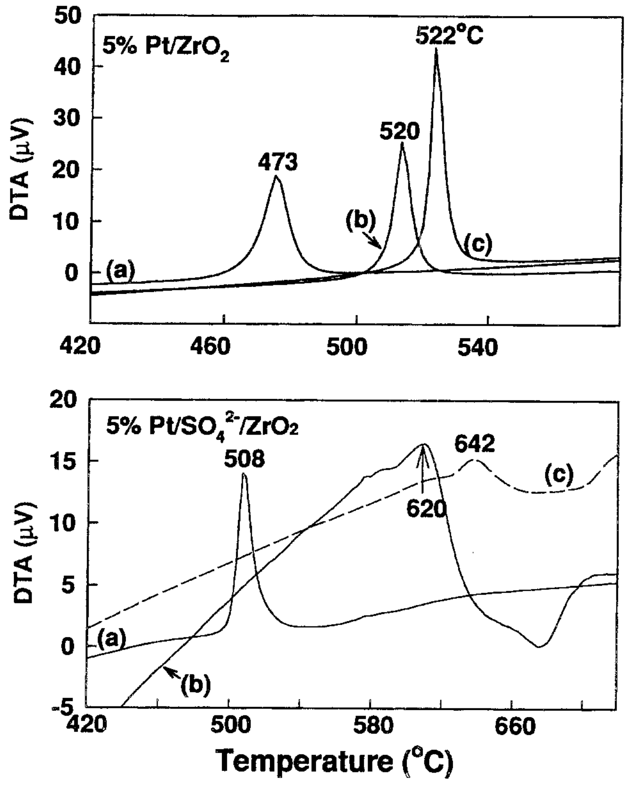

Fig. 1. DTA curves for the 5 wt% Pt/ZrO_2 (top) and 5 wt% $Pt/SO_4^{2-}/ZrO_2$ catalysts heated (a) in H_2, (b) in helium, and (c) in air.

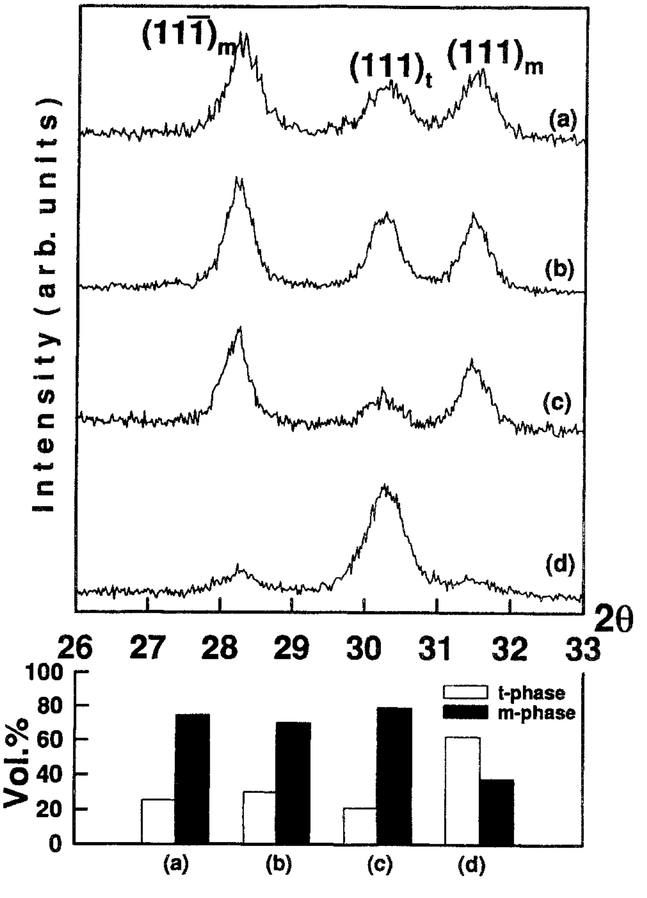

Fig. 2. XRD pattern (top) obtained from the 5 wt% Pt/ZrO_2 catalyst after: (a) activation in air at 725°C for 2 h, (b) reduction in H_2 at 725°C for 6 h, (c) activation in air at 725°C for 2 h and then reduction in H_2 at 725°C for 6 h, and (d) reduction in H_2 at 450°C for 6 h. The vol% m- and t-phases are shown at the bottom.

Table 1
Volume fraction of crystalline phases in the 5 wt% Pt/ZrO_2 catalysts

Catalyst	% m-phase	% t-phase
activated in air at 725°C for 2 h	74.5	25.5
reduced in H_2 at 725°C for 6 h and passivated	70.0	30.0
activated in air for 2 h and then reduced in H_2 for 6 h, both at 725°C and passivated	79.0	21.0
reduced at 450°C for 6 h and passivated	38.0	62.0

642°C (in air), 620°C (in He), and 508°C (in H_2). The exotherm temperature increases in the order: $H_2 >$ He $>$ air. For the Pt/ZrO_2 sample, these exotherms occur at lower temperatures: 522, 520 and 473°C for air, helium and hydrogen, respectively.

The XRD patterns obtained from the 5 wt% Pt/ZrO_2 (without sulfur) (fig. 2) for the 2θ region of 26–32° show the extent of the formation of t- and m-phases, and their transformation from one to the other (table 1). It is evident that after activation in air at 725°C the predominant ZrO_2 phase is monoclinic (75% m-phase and 25% t-phase). After reduction at 725°C in H_2 for 6 h, again, a

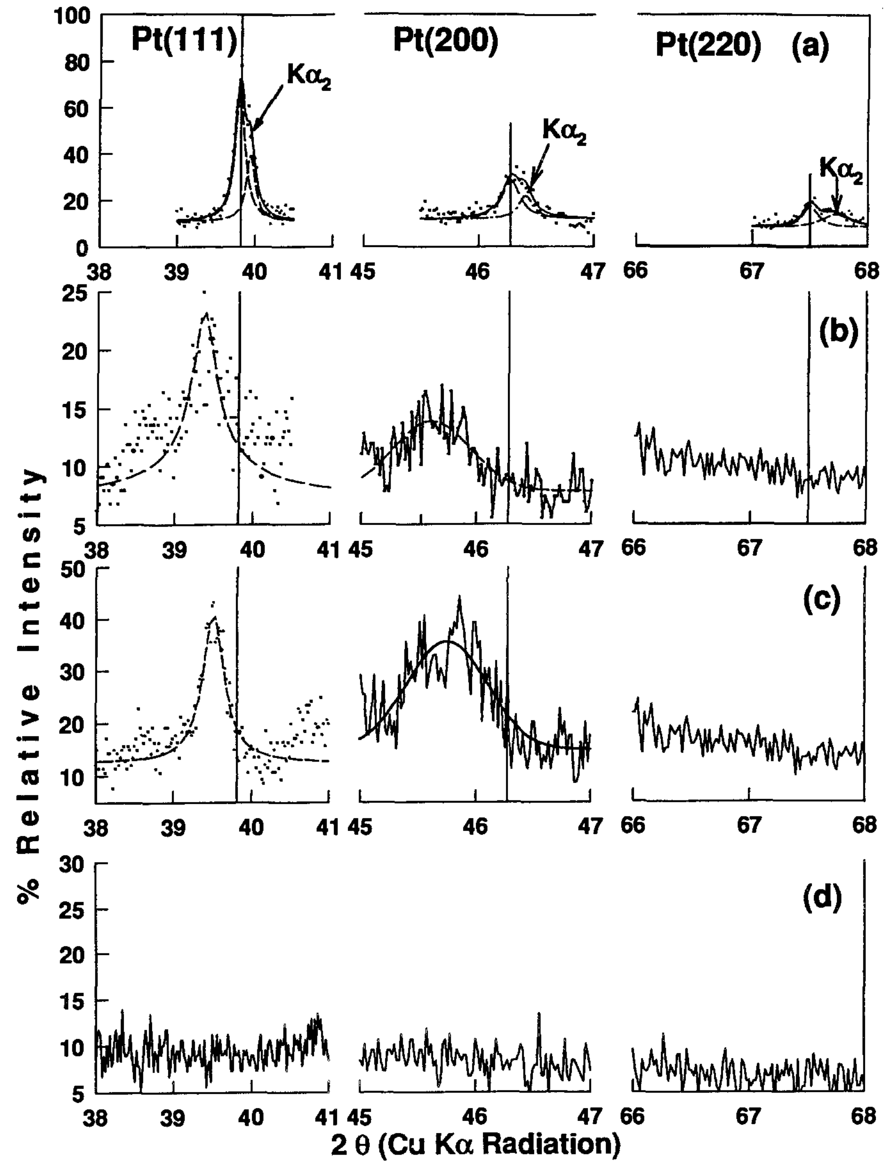

Fig. 3. XRD patterns for the 5 wt% Pt/ZrO_2 catalyst for the (111), (200) and (220) Pt peaks: (a) after activation in air at 725°C for 2 h, (b) after reduction in H_2 at 725°C for 6 h, (c) after activation in air at 725°C for 2 h and subsequent reduction in H_2 at 725°C for 6 h, and (d) after reduction in H_2 at 450°C for 6 h.

Table 2
Particle size data calculated from the half-width at maximum intensity from Pt(111) profile (nm)

	Catalyst	
	5 wt% Pt/ZrO_2	5 wt% $Pt/SO_4^{2-}/ZrO_2$
activation in air at 725°C for 2 h	36.5	33.8
reduction in H_2 at 725°C for 6 h and passivation	13.3	7.0
activation in air at 725°C for 2 h and subsequent reduction at 725°C in H_2 and passivation	19.5	16.5
reduction in H_2 at 450°C for 6 h and passivation	[a]	[a]

[a] Could not be determined.

mixture of m- and t-phases is present. After activation at 725°C for 2 h and subsequent reduction at this temperature for 6 h in H_2, the % m-phase increases slightly. This phase transformation phenomenon was extensively discussed in earlier communications [16,20] in which adsorption of oxygen on ion vacancies on the surface of zirconia was considered to trigger the phase transformation. The predominant phase for the catalyst reduced at 450°C for 6 h was the t-phase.

The 2θ regions for the three prominent Pt peaks [(111), (200) and (220)] for the 5 wt% Pt/ZrO_2 (sulfur free) catalyst are presented in fig. 3. This catalyst, after activation at 725°C in air, clearly exhibits the metallic Pt peaks (fig. 3a) with a crystallite size of approximately 36 nm (table 2). In fig. 3 the Pt (111), (200) and (220) peaks from JCPDS file #4-820 are superimposed. It is therefore clear that metallic platinum is formed after calcination at 725°C for 2 h in air. The 2θ regions corresponding to the three Pt peaks are shown in fig. 3b for the catalyst after reduction at 725°C for 6 h and subsequent passivation and are in marked contrast to the data in fig. 3a. After reduction at 725°C, the positions of the peaks are shifted, indicating an increase in lattice parameters. The lattice parameters of Pt do not increase in hydrogen environment. Therefore, this indicates that a Pt–Zr alloy is present, following reduction treatment at 725°C, and this agrees with an earlier report of Pt–Zr alloy formation [21,22]. The XRD pattern for the catalyst after activation in air at 725°C for 2 h and subsequent reduction at 725°C for 6 h (fig. 3c) also indicates that a Pt–Zr alloy is formed in this case. However, after reduction at 450°C for 6 h, metallic Pt is not detectable (fig. 3d). Therefore, the following points can be noted from the data in fig. 3: (a) metallic platinum crystallites of about 36 nm in diameter are formed after activation in air at 725°C for 2 h, (b) some Pt–Zr alloy is formed following reduction at 725°C, and (c) reduction at 450°C produces a dispersion so high that XRD cannot detect metallic platinum.

The XRD patterns in the 2θ region of 26–33° (fig. 4) for the 5 wt% $Pt/SO_4^{2-}/ZrO_2$ indicate that they were predominantly the tetragonal phase. This is consistent with the view that the presence of sulfate appears to stabilize the tetragonal phase (e.g., ref. [23]). The sample reduced at 725°C for 6 h showed higher content of the m-phase than the other samples, and this is consistent with the loss of more sulfur during the hydrogen treatment.

The 2θ regions (Cu Kα radiation) of the Pt (111), (200) and (220) profiles are plotted in fig. 5 for the 5 wt% $Pt/SO_4^{2-}/ZrO_2$ catalyst. It can be seen that after activation in air at 725°C for 2 h, metallic Pt is formed, and this is evident from fig. 5a, wherein Pt (111), (200) and (220) profiles from JCPDS file #4-820 are superimposed. It is clear that after activation in air, large crystallites of platinum (~ 36 nm) are formed, as determined by the half-width at maximum intensity [24] (see fig. 5a). The three prominent Pt profiles for the catalyst which is reduced in

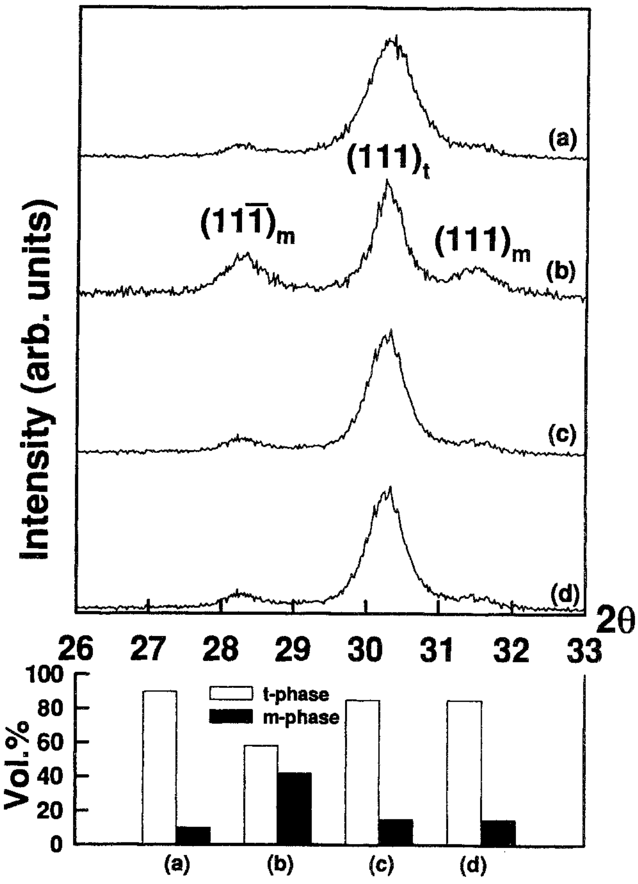

Fig. 4. XRD patterns obtained from the 5 wt% $Pt/SO_4^{2-}/ZrO_2$ catalyst after: (a) activation at 725°C for 2 h in air, (b) reduction in H_2 at 725°C for 6 h, (c) after activation at 725°C for 2 h in air and subsequent reduction on H_2 at 725°C for 6 h, and (d) after reduction in H_2 at 450°C for 6 h.

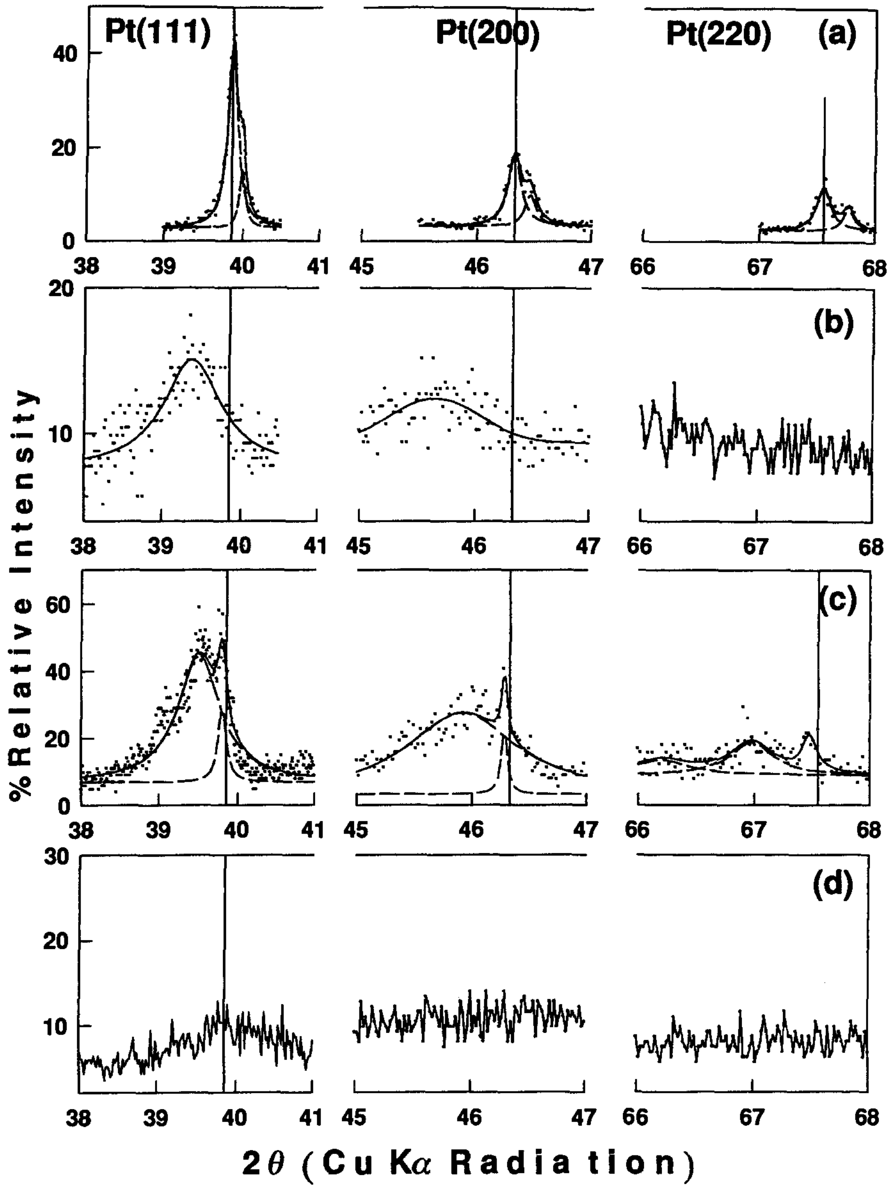

Fig. 5. XRD patterns obtained from the 5 wt% Pt/SO_4^{2-}/ZrO_2 catalyst after: (a) activation at 725°C for 2 h, (b) reduction in H_2 at 725°C for 6 h, (c) activation at 725°C for 2 h and subsequent reduction at 725°C for 6 h, and (d) reduction at 450°C for 6 h.

H_2 at 725°C for 6 h and subsequently passivated are shown in fig. 5b, and these data are in contrast to the data in fig. 5a. None of the peaks correspond to platinum but are consistent with a Pt–Zr alloy. This is more evident in fig. 5c, in which the three peaks are shown for the catalyst following activation in air and subsequent reduction in hydrogen at 725°C. The data in fig. 5c clearly indicate that some large crystallites of metallic platinum formed during activation in air at 725°C remain, while some fraction of platinum forms an alloy with Zr. The complete conversion of metallic platinum to alloy depends upon the period of reduction at 725°C, and perhaps on the presence of the sulfur species. After reduction at 450°C, the peaks are so broad that the presence of metallic platinum could not be discerned (fig. 5d).

The X-ray diffraction patterns for the metallic platinum for the 5 wt% Pt/ZrO_2 without any sulfate ions (fig. 3) clearly indicate that metallic platinum was formed after activation in air at 725°C for 2 h even in the absence of sulfur species. Fig. 5 illustrates the same result for the 5 wt% Pt/SO_4^{2-}/ZrO_2 catalyst. This demonstrates that the platinum species are reduced to the metal even in the absence of sulfur.

The 0.6% Pt/SO_4^{2-}/ZrO_2 was used as a catalyst for methylcyclohexane (MCH) conversion. After activation in air at 725°C for 2 h, this catalyst was transferred into a batch reactor and the reactor was sealed. The conversion of MCH was carried out at 150°C at 500 psig for 15 min. After this reaction period, the catalyst was removed from the reactor and was subjected to characterization studies. The X-ray diffraction pattern obtained from this catalyst indicated the same phases as the sample activated at 725°C for 2 h. This suggests that the reactions carried out at lower temperatures do not significantly alter the structural characteristics formed after activation at 725°C.

It appears that if a Pt–Zr alloy is formed, recalcination in air of the H_2 reduced sample should cause reoxidation of the Pt–Zr alloy to form ZrO_2 and Pt. Therefore, the catalyst which was reduced at 725°C for 6 h was calcined at 725°C for 2 h in air. This recalcination treatment was also given to the 5 wt% Pt/ZrO_2 catalyst, which was first activated at 725°C for 2 h in air and subsequently reduced at 725°C for 6 h. The XRD patterns obtained from these recalcined samples (fig. 6) clearly demonstrate that, after recalcination at 725°C, the Pt that was present as an alloy with Zr again forms Pt crystallites. The 5 wt% Pt/ZrO_2 sample, after activation in air at 725°C, was reduced in H_2 at 150 or 450°C and the XRD patterns (fig. 7) indicate that these reductions did not cause any increase in the lattice parameters. However, reduction at 725°C caused a dramatic shift in the lattice parameters. This suggests that Pt–Zr alloy is formed only when the sample is reduced above a temperature of 450°C for 6 h. XRD patterns for different Pt phases, such as PtS or oxides of platinum could not be detected.

Darling et al. [21] provide data for the lattice spacings of Pt_xZr alloys, and these data have been used to produce a linear calibration curve relating the d-spacing to the atomic fraction of Zr (0–12 at% Zr) in the alloy. This calibration curve was then utilized together with the d-spacings for the XRD curves in figs. 3b, 3c, 5b, 5c, 6a, 6c and 7d to calculate the Pt–Zr alloy composition of the materials indicated above. The direct reduction in H_2 at 725°C of the Pt/ZrO_2 sample led to an alloy with 4.2 at% Zr (fig. 3b); when the sample was first calcined in air at 725°C for 2 h and then reduced in H_2 at 725°C the at% Zr in the alloy was 2.8%. When the Pt/SO_4^{2-}/ZrO_2 sample was treated the same as the Pt/ZrO_2 catalyst, similar results were obtained. Thus, following H_2 reduction of the Pt/SO_4^{2-}/ZrO_2 sample, the alloy contained 4.3 at% Zr (fig. 5b) whereas the calcined and reduced sample had 2.8 at% Zr alloy. The alloy compositions in figs. 6 and 7 are also very similar to those for the samples shown in figs. 3 and 5: 6a is 4.2 at% Zr; 6c is 2.8 at% Zr; and 7d is 2.8 at% Zr. It appears that the rate of reduction permits a similar extent of alloy formation under similar reduction conditions.

The crystalline phases developed in the catalysts are quite stable following the passivation step. XRD diffraction patterns obtained from the passivated catalysts, which were stored for 2–3 months, were the same as those obtained just after reduction treatment and subsequent passivation step.

It is apparent that ZrO_2 is capable of being reduced under severe conditions for short time periods, and this can lead to the formation of Pt–Zr alloy. There have been similar reports for the reduction of Al_2O_3 and the formation of Pt–Al alloys under severe reducing conditions. The reduction treatment under severe conditions suggests the generation of Lewis acid sites under less severe conditions should be possible and this provides an additional factor in considering the nature of the active sites in these Pt/SO_4^{2-}/ZrO_2 catalysts.

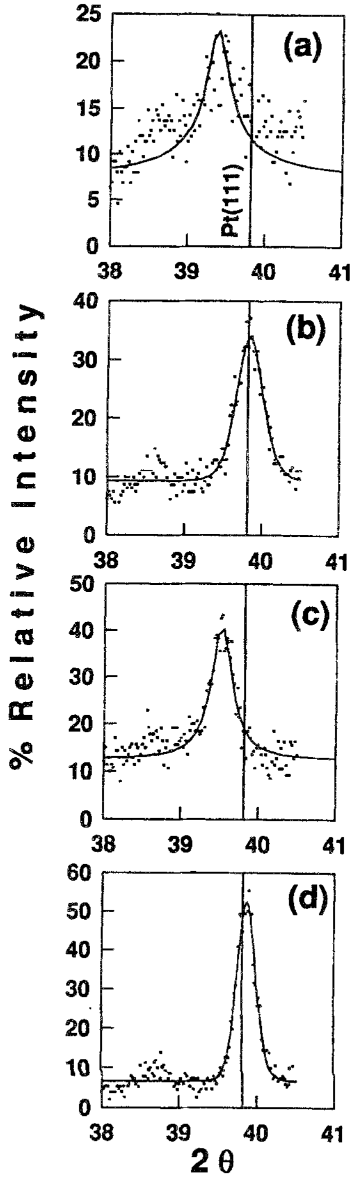

Fig. 6. XRD patterns obtained from the 5 wt% Pt/ZrO_2 catalysts in the 2θ regions of 38–41° covering Pt (111) profile after: (a) reduction in H_2 at 725°C for 6 h followed by passivation; (b) recalcination of the above sample in air at 725°C for 2 h; (c) activation in air at 725°C for 2 h followed by reduction in H_2 at 725°C for 6 h and subsequent passivation; and (d) recalcination of the above sample in air at 725°C for 2 h. Similar data were obtained for the 5 wt% Pt/SO_4^{2-}/ZrO_2 catalysts.

4. Conclusions

The present data demonstrate that platinum is present in the metallic state after activation in air at 725°C.

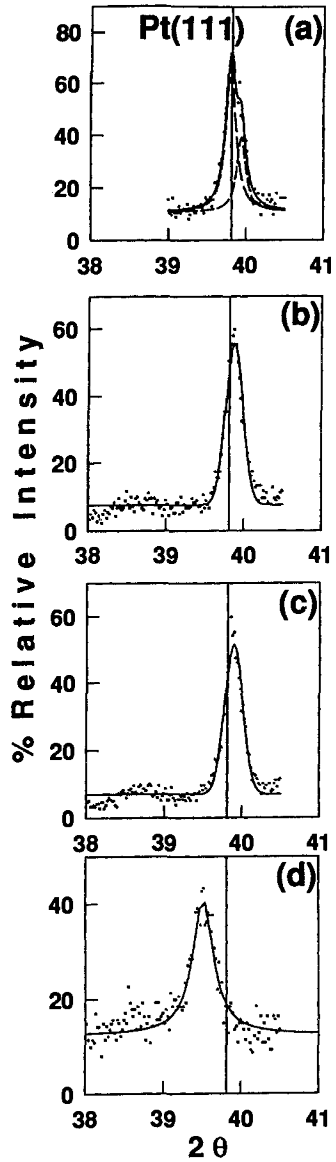

Fig. 7. XRD patterns obtained from the 5 wt% Pt/ZrO_2 sample after: (a) activation in air at 725°C for 2 h; (b) activation in air at 725°C for 2 h followed by reduction in H_2 at 150°C for 6 h and subsequent passivation; (c) activation in air at 725°C for 2 h, followed by reduction in H_2 at 450°C for 6 h and subsequent passivation; and (d) activation in air at 725°C for 2 h followed by reduction in H_2 at 725°C for 6 h and passivation. Note that significant amounts of Pt–Zr alloy are formed only after reduction at 725°C, and not after 150°C or 450°C reduction.

The appearance of metallic platinum in air is simply due to a reductive decomposition of H_2PtCl_6, the salt used for impregnation, and not due to the presence of sulfur species. Treatment in hydrogen at 725°C forms a Pt–Zr alloy. Thus, the XRD patterns from the 0.6 and 5 wt% Pt/SO_4^{2-}/ZrO_2 indicate that metallic Pt particles are present after activation in air at 725°C for 2 h; this Pt forms an alloy with Zr after reduction in H_2 at 725°C for 6 h. This alloy, upon recalcination in air, is converted again to metallic Pt and ZrO_2, indicating that this is a reversible reaction.

Acknowledgement

This work was supported by the DOE contract #DE-AC22-90PC90049 and the Commonwealth of Kentucky.

References

[1] K. Arata, Adv. Catal. 27 (1990) 165.
[2] T. Yamaguchi and K. Tanabe, Mater. Chem. Phys. 16 (1986) 67.
[3] E.J. Hollstein, J.T. Wei and C.-Y. Hsu, US Patent 4,918,041, 17 April, 1990.
[4] B. Davis, R.A. Keogh and R. Srinivasan, Catal. Today 20 (1994) 219.
[5] T. Hosoi, T. Shimadzu, S. Ito, S. Baba, H. Takaoka, T. Imai and N. Yokoyama, Prepr. Symp. Div. Petr. Chem. Am. Soc. 562 (1988).
[6] K. Ebitani, J. Konishi and H. Hattori, J. Catal., 130 (1991) 257.
[7] T. Huizinga and R. Prins, in: *Metal–Support and Metal–Adsorptive Effects in Catalysis*, Studies in Surface Science and Catalysis, Vol. II, eds. B. Imelik, C. Naccache, G. Coudurier, H. Praliaud, P. Meriaudeau, P. Gallezot, G.A. Martin and J.C. Vedrine (Elsevier, Amsterdam, 1982) p. 11.
[8] T. Huizinga, H.F.J. van't Blik, J.C. Vis and R. Prins, Surf. Sci. 135 (1983) 580.
[9] Y. Takasu, R. Unwin, B. Tesche, A.M. Bradshaw and M. Grumze, Surf. Sci. 77 (1978) 219.
[10] H.F.J. van't Blik, J.B.A.D. van Zon, T. Huizinga, J.C. Vis, D.C. Koningsberger and R. Prins, J. Am. Chem. Soc. 107 (1985) 3139.
[11] K. Ebitani, H. Konno, T. Tanaka and H. Hattori, J. Catal. 135 (1992) 60.
[12] Z. Paál, M. Muhler and R. Schlögl, J. Catal. 143 (1993) 318.
[13] E. Iglesia, S.L. Soles and G. Kramer, J. Catal. 144 (1995) 238.
[14] K. Ebitani, H. Konno, T. Tanaka and H. Hattori, J. Catal. 143 (1993) 322.
[15] A. Sayari and A. Dicko, J. Catal. 145 (1994) 561.
[16] R. Srinivasan, O.B. Cavin, C.R. Hubbard and B.H. Davis, J. Am. Ceram. Soc. 75 (1992) 1217.
[17] K. Ebitani, T. Tanaka and H. Hattori, Appl. Catal. A 102 (1993) 79.
[18] J. Zhao, G.P. Huffman and B.H. Davis, Catal. Lett. 24 (1994) 385.
[19] R. Srinivasan and B.H. Davis, Catal. Lett. 14 (1992) 165.
[20] R. Srinivasan, T.R. Watkins, C.R. Hubbard and B.H. Davis, Chem. Mater. 7 (1995) 725.
[21] A.S. Darling, G.L. Selman and R. Rushforth, Plat. Metals Rev. 14 (1970) 14.
[22] R. Szymanski and H. Charcosset, Plat. Metals Rev. 30 (1986) 23.
[23] R. Srinivasan, D. Taulbee and B.H. Davis, Catal. Lett. 9 (1991) 1.
[24] H.P. Klug and L.E. Alexander, *X-ray Diffraction Procedure* (Wiley, Chichester, 1967) p. 491.